

Lanthanide-doped Upconversion Nanoparticles for Emerging Applications in Drug Delivery and Therapeutics

ELISABETH DUIJNSTEE*

Zernike Institute for Advanced Materials, University of Groningen
Supervisor: Dr. A. Salvati[†], Second supervisor: Prof. A. Herrmann[‡]

March 29, 2017

Abstract

Lanthanide-doped upconversion nanoparticles, in which the sequential absorption of two or more low-energy photons leads to the emission of a higher-energy photon under excitation by near-infrared light, have showed an impressive array of potential applications in many different fields, including biomedicine. The upconverted luminescence exhibits improved tissue penetration depth, higher photochemical stability, sharp and tunable emission peaks, high resistance to photobleaching and minimized background autofluorescence, compared to traditional downconversion luminescent biolabels. Moreover, surface syntheses and modifications can provide functional groups to enrich the properties of the upconversion nanoparticles. The unique upconversion process of lanthanide-doped upconversion nanoparticles can be utilized for drug delivery and photoactivated release of therapeutic agents, as well as for applications in therapy for cancer treatment. This review will first describe mechanisms for upconversion emission and properties of upconversion nanoparticles. Then, it will focus on the composition, synthesis and bioconjugation of the upconversion nanoparticles, and the applications for drug delivery and therapy are examined. Finally, the recent advances and future prospects in this emerging field are discussed. It is found that thorough development on several aspects like quantum yield, toxicity and reproducible synthetic approaches would allow the applications of upconversion nanoparticles to potentially go to clinical use.

CONTENTS

	ii	Photothermal therapy	10
	iii	Lanthanide nanocomplexes in other therapy forms	12
I Introduction	1		
II Mechanisms for upconversion emission	2		
III Properties of upconversion nanoparticles	3		
i Composition	3		
ii Optical properties	4		
iii Quantum yield	5		
IV Synthesis, surface modification and bioconjugation of upconversion nanoparticles	6		
i Synthesis	6		
ii Surface modification	6		
iii Bioconjugation	7		
V Upconversion nanoparticles for biomedical applications	7		
i Drug delivery	7		
i <i>In vitro</i> and <i>in vivo</i> photoactivation	9		
ii Phototherapy	9		
i Photodynamic therapy	9		
		VI Remaining challenges for lanthenide-doped upconversion nanoparticles	13
		i Quantum yield and extinction coefficient	13
		ii Toxicity and biodegradability	14
		VII Summary and future directions	15
		VIII Acknowledgements	15
		References	15

I. INTRODUCTION

Photon upconversion is a nonlinear optical phenomenon which was proposed as a theoretical concept by Bloembergen in 1959.¹ It is an anti-stokes emission where the sequential absorption of two or more low-energy photons via excited states absorption (ESA) leads to the luminescence emission of a high-energy photon.² Despite his pioneering work in nonlinear optics, he was not able to validate his idea as a consequence of the lack of coherent pumping sources.

*Email: e.a.duijnstee@student.rug.nl, Studentnumber: S2542846

[†]Department of Pharmacokinetics, Toxicology and Targeting, University of Groningen

[‡]Zernike Institute for Advanced Materials, University of Groningen

Francois Auzel was the first to establish the validity in 1966, by reporting energy transfer upconversion (ETU).³

Conventional fluorophores like quantum dots, organic fluorophores and fluorescent proteins, which usually emit a lower-energy photon after absorption of a high-energy photon, have been widely exploited for biomedical applications such as sensing, labeling, detection, imaging and therapy. Yet, they are associated with several drawbacks like autofluorescence, high toxicity and low chemical stability.⁴

Recently, the upconversion phenomena have gained increasing attention because of the widespread research on nanomaterial synthesis, in conjunction with the pressing demand in the interdisciplinary fields of biology and nanoscience. Lanthanide (Ln^{3+})-doped upconversion nanoparticles (UCNPs), which can emit high-energy photons in the ultraviolet/visible after absorbing two or more low-energy photons, demonstrated to have excellent properties for biomedical applications due to the sharp emission peaks,⁵ absence of autofluorescence, photobleaching and chemical degradation under near-infrared (NIR) radiation,^{6,7} great signal-to-background ratio,⁸ long luminescence lifetime and large Stokes-shift.⁹ Also the low-cost NIR excitation light and deep penetration depth favours the use of UCNPs.⁹

As there are several comprehensive reviews published about lanthanide-doped UCNPs for bioimaging and biosensing applications, this review will focus on the recent applications in drug delivery and therapeutics.⁹⁻¹² First, a brief introduction to the fundamental aspects of upconversion will be given, followed by the composition and optical properties of upconversion nanoparticles. Then a description of the synthesis, functionalization and bioconjugation of UCNPs is given. Next, emphasis is placed on the application of UCNPs in drug delivery and therapy in biomedical applications. The following section highlights the remaining challenges for improving the properties of UCNPs. Finally, a summary and a personal view of future perspectives for research in this area will be given.

II. MECHANISMS FOR UPCONVERSION EMISSION

The upconversion (UC) mechanisms can roughly be categorized into four classes according to recent advances: excited-state absorption (ESA),³ energy transfer upconversion (ETU),³ photon avalanche (PA),¹⁴ and energy migration-mediated upconversion (EMU),¹³ which was more recently developed.¹² The different upconversion processes are shown in figure 1. In figure 1a, b, and c, I and II are the sensitizer and activator, respectively. In figure 1d, I, II III & IV, are the sensitizer, accumulator, migrator and activator, respectively. All processes

are based on the sequential absorption of two or more photons by metastable, long-lived energy states. The sequential absorption then leads to the upconversion emission from a highly excited state.¹⁵ It should be noted that the upconversion emission is strongly dominated by the ETU process and that ETU and EMU are mostly used for applications in drug delivery and therapeutics, as shown in section 5.

In a typical ESA process (figure 1a), the absorption of a low-energy photon leads to the electron transition from the ground state to a metastable intermediate state.¹⁶ A second pump photon then leads to the excitation of the excited electrons to a higher excited state. When the electrons radiatively fall back into their ground state, UC emission occurs.

ETU (figure 1b), is different from ESA as ETU involves two neighboring ions in stead of one lanthanide ion, like in ESA. So, in ETU there are two types on luminescent centres: the sensitizer and the activator, both embedded in a host matrix. Upon excitation of low-energy photons, the sensitizer is excited from the ground state to its metastable energy level. Afterwards, it transfers its harvested energy to the activator. As a consequence of the non-radiative energy transfer from the sensitizer to the activator, there is sequential absorption of the activator to the higher excited state, while the sensitizer relaxes back to the ground state. Radiative emission in the activator back to the ground state can then be observed as UC emission.¹⁶ The efficiency of this UC process is determined by the distance between the sensitizer and the activator (r_{s-a}), which is determined by the concentration of the dopants, and the overlap of the spectra.¹⁷ In addition, for efficient ESA and ETU, a ladder-like arrangement of the energy states is required to minimize relaxation losses and to facilitate absorption. Of course, high absorption at the emission wavelength of the sensitizer is required.

Under certain conditions, there is a unique UC process that is based on the combination of the above two mechanism called photon avalanche (PA), as shown in figure 1c. In order for PA to occur, the pumping energy must be larger than the absorption energy of the intermediate level (E1) ($E_{\text{pump}} > E1 - G$) for the population of E1 through non-resonant transitions, and the difference in energy between the excited state (E2) and the intermediate energy levels (E1) must be resonant with the energy of the pumping system ($E_{\text{pump}} = E2 - E1$). Also, there must be an efficient cross-relaxation process, where the activator transfers part of its excited energy to the sensitizer. Above a certain pump threshold, there is an increase in the number of active ions that populate the intermediate metastable energy level of the activator, and then the photon avalanche process may start. The competition between intensity gain and intensity losses gives rise to an enhancement of the upconverted emission from the excited level. Again, the efficiency

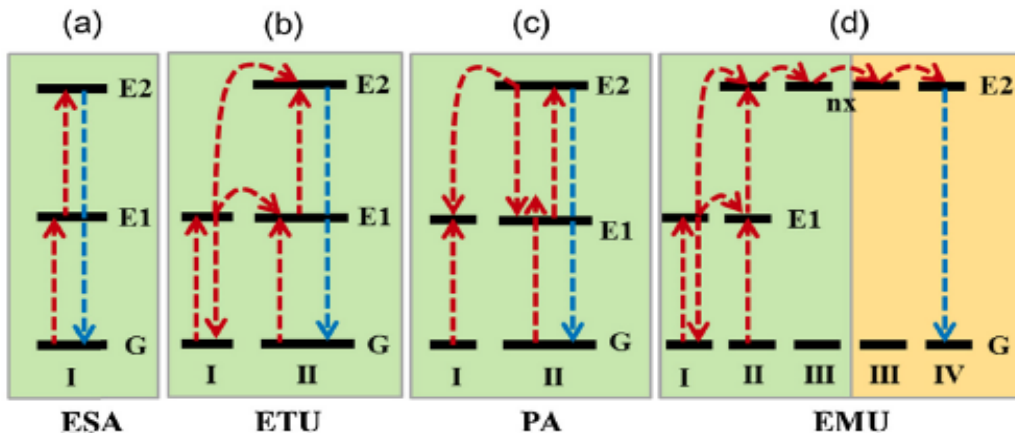


Figure 1: Principal UC processes for lanthanide-based UCNPs: (a) ESA, (b) ETU, (c) PA, (d) EMU. Note that core and shell regions are highlighted with different background colors. The red arrows represent photon excitation and energy transfer. The blue arrows represent the emission processes.¹³

of this process is strongly related to the concentrations of the dopants. Nevertheless, PA is rarely observed in UCNPs, as it requires a pump threshold and a long time (seconds) to build up.¹⁸

The fourth process, EMU, is a quite complicated process proposed by Wang *et al.*¹³ In the EMU process (figure 1d), a sensitizer is used to harvest the pump photons and then promote a neighbouring accumulator to the excited state. This excitation energy is then extracted from high-lying energy states of the accumulator. Afterwards, there is random energy hopping through the migrator ion sublattice and trapping of the migrating energy by an activator. The sensitizer/accumulator and the activator are spatially confined in different layers of a core-shell structure to regulate the energy exchange interaction between the accumulator and the activator. Several migrator ions through the core-shell interface are required for an efficient EMU process to bridge the transfer of energy from the accumulator to the activator.¹³

III. PROPERTIES OF UPCONVERSION NANOPARTICLES

For efficient upconversion to proceed, the composition and optical properties of UCNPs should be well understood.

i. Composition

As explained, luminescent materials featuring f- and d-ions and containing more than one intermediate energy level, can in principle be used for generation of UC luminescence. However, efficient UC processes mostly occur in lanthanide-doped UCNPs because of their extremely long-lived intermediate energy states.¹¹ Lanthanides are rare earth elements, with an electronic

structure that has the ability to emit with higher energy than the excitation energy. The lanthanides $4f^n$ ($n=0-14$) electron configurations are split by electronic repulsion and spin-orbit coupling as shown in figure 2. This leads to a splitted energy level pattern, where the energy levels can act as energy reservoirs, which is required for efficient UC.¹⁹

As mentioned before, in the dominated ETU process, Ln^{3+} -doped UCNPs are composed of three different components, namely a host matrix, a sensitizer and an activator, where the sensitizer can effectively be excited by the incident light source and can transfer its energy to the activator, which in its turn emits the radiation.³ Optical emissions under low pump power densities are only generated by using Er^{3+} , Tm^{3+} and Ho^{3+} as activator, as they have equally spaced energy levels, which minimize irradiative losses and facilitate absorption and energy transfer.^{8,20} An often used sensitizer is Yb^{3+} , as it contains a large absorption cross section in the NIR. Other sensitizers may be used to enhance of quench specific emission bands. The sensitizer and activator are added to the host lattice in low concentrations (about 20% for the sensitizer and less than 2% for the activator), as this allows for a good distance between the activator and the sensitizer without having cross-relaxations but with enough absorption for the sensitizer to be efficient.¹⁰

For the realization of an efficient UC process, the host material plays an important role in terms of crystal structure and optical properties. The host material should desirably have low phonon energy to suppress vibrational relaxation and to increase the lifetime of the intermediate states, adequate transparency in the interested energy range to minimize scattering losses, and it should be chemically stable. The crystal field of the host material has a large effect on the UC efficiency of the lanthanide-doped nanoparticles. Depending on

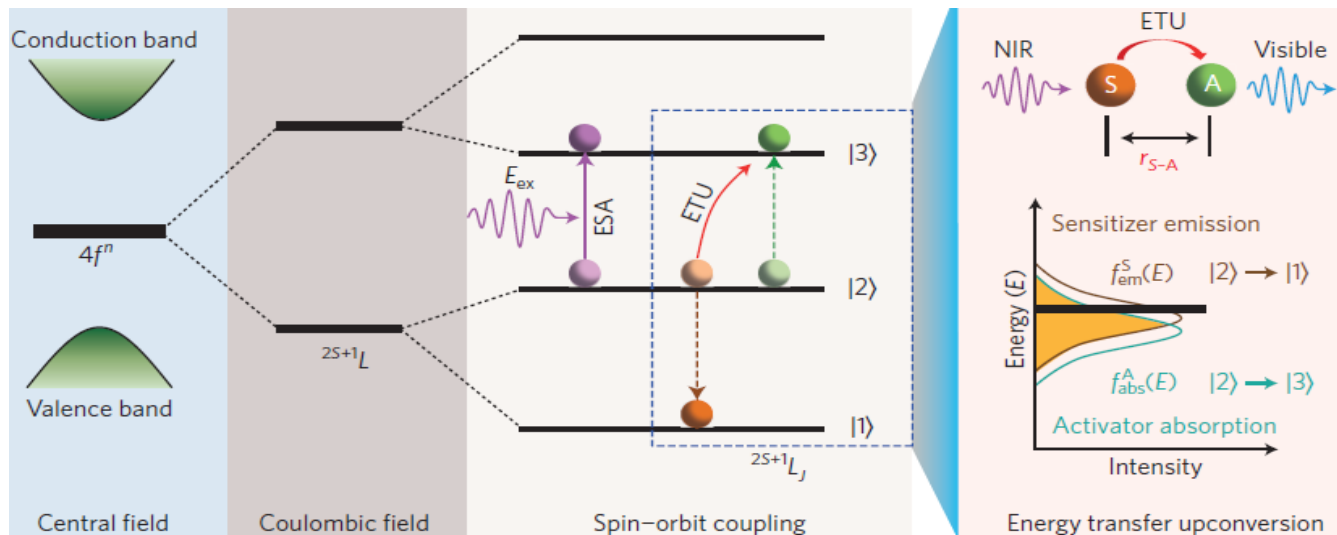


Figure 2: Electronic energy level diagrams of Ln^{3+} ions in relation to upconversion processes. The $4f^n$ electronic configurations splits into many energy sublevels due to the strong effects of the Coulombic interaction and spin-orbit coupling as well as weak crystal-field perturbation. The energy levels are represented by the symbol $^{2S+1}L_J$ (where S , L , J are the total spin, orbital and angular momentum quantum number of the electron, respectively), and optical transitions among these energy levels lead to abundant emission bands. In principle, a Ln^{3+} ion residing in an intermediate level $|2\rangle$ can be further promoted to an upper emitting level $|3\rangle$ through absorption of another photon E_{ex} (ESA process), or through cooperative energy transfer between a pair of excited ions with one ion being non-radiatively decayed to the ground state $|1\rangle$ (ETU process). The right inset panel shows that the realization of an efficient ETU process requires consideration of the sensitizer-activator distance (r_{S-A}), and the spectral overlap between sensitizer emission ($f_{\text{em}}^S(E)$) and activator absorption ($f_{\text{abs}}^A(E)$) profiles.¹⁹

the symmetry of the crystal field, the optical properties are influenced.¹¹ In order to achieve high doping levels, the host lattice should have close lattice matches to dopant ions to readily incorporate Ln^{3+} dopant ions.¹⁰ Fluoride based lattices, such as LaF_4 , YF_4 , NaYF_4 and BaYF_4 , have been employed extensively as host lattice as they meet many of the above named criteria.^{9,21} To date, the most efficient mono dispersed core-shell UCNPs which produce green and blue emissions are $\text{Yb}^{3+}/\text{Er}^{3+}$ and $\text{Yb}^{3+}/\text{Tm}^{3+}$ doped in hexagonal phase NaYF_4 ($\beta\text{-NaYF}_4$).^{22,23} The greater UC emission of $\beta\text{-NaYF}_4$ made this composition more preferable than the cubic form $\alpha\text{-NaYF}_4$ which is the composition at lower temperatures. Thermal treatment at ca. 400-600 °C transforms the cubic phase to the hexagonal phase.²⁴ $\alpha\text{-NaYF}_4$ was the first composition used for the demonstration of tunable color UC luminescence from green to red.²⁵ It was proven that a less symmetric crystal phase is more favourable for the UC efficiency, as it allows for intermixing of the lanthanide ion its f states with higher electronic configurations.^{11,25,26}

The energy level diagrams of the most common lanthanide sensitizer/activator combinations employed for UC (combinations of Yb^{3+} and $\text{Er}^{3+}/\text{Tm}^{3+}/\text{Ho}^{3+}$) are shown in figure 3. It shows that under 980 nm irradiation, $\text{Yb}^{3+}/\text{Er}^{3+}$ gives green and red emissions at 525 nm ($^4I_{15/2}\text{-}^2H_{11/2}$) and 655 nm ($^4I_{15/2}\text{-}^4F_9/2$) respectively, after the absorption of two photons. The populations of the energy levels undergo changes under the excitation of different power densities, so increasing

the pumping power can give violet-blue emissions at 415 nm ($^2H_{9/2}\text{-}^4I_{15/2}$), which is a three- or four-photon emission process.^{27,28} $\text{Yb}^{3+}/\text{Tm}^{3+}$ results in ultra-violet (UV) emission at 360 nm ($^1D_2\text{-}^3H_6$), blue emissions at 450 nm ($^1G_4\text{-}^3H_6$) and 475 nm ($^1G_4\text{-}^3H_6$), red emissions at 650 nm ($^1G_4\text{-}^3F_4$) and at 695 nm ($^3F_2\text{-}^3H_6$) and IR emission at 800 nm ($^3H_4\text{-}^3H_6$). Emissions at 695 nm and 800 nm are two-photon processes, while emissions at 475 nm and 650 nm are three-photon processes and emissions at 360 nm and 450 nm are four-photon processes, meaning that these emissions occur when respectively two, three or four photons are absorbed. $\text{Yb}^{3+}/\text{Ho}^{3+}$ complexes give red emission at 645 nm ($^5F_5\text{-}^5I_8$), green emission at 542 nm ($^5S_2\text{-}^5I_8$) and blue emission ($^5F_3\text{-}^5I_8$).¹²

ii. Optical properties

In comparison to traditional fluorescent biolabels, lanthanide-doped UCNPs can be excited by an inexpensive, low-power NIR excitation source and possess several advantages such as sharp emission peaks, long photoluminescence lifetime, larger anti-stokes shift, high resistance to photobleaching, chemical degradation and photoblinking, good signal-to-background ratio and improved sensitivity as a consequence of the absence of autofluorescence, as mentioned in the introduction. Along with deeper NIR light penetration into the tissue which reduces the photodamaging of the tissue, UCNPs are ideal for usage as alternatives to conven-

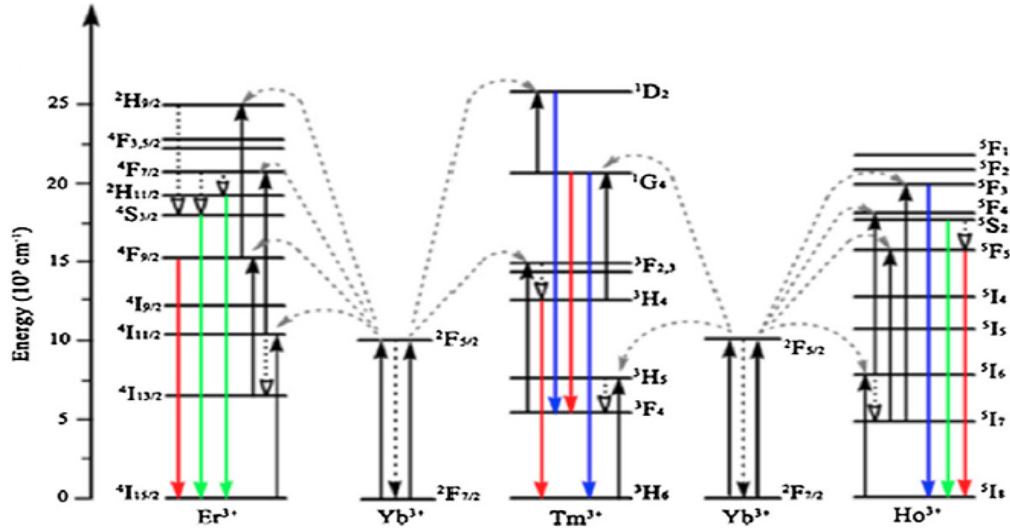


Figure 3: Energy level diagrams and energy transfer process in Yb^{3+} , $\text{Er}^{3+}/\text{Tm}^{3+}/\text{Ho}^{3+}$.¹²

tional biolabels. This section will focus on the optical properties of lanthanide-doped UCNPs.

The shielding of the partially filled 4f orbitals by the outer 5s and 5p shells of the lanthanide ions, results in a distinct set of sharp emission peaks, which makes accurate interpretation of the spectra possible.^{5,11,29} Tuning the host/dopant combinations, dopant concentration, particle size, surface ligands and crystallinity enables emission manipulation.¹¹ Each lanthanide ion can produce distinct sharp emission peaks. So a selection of different lanthanide ions, or combinations of them, enables the production of multicolour emission and their relative emission intensities.^{11,30} Changing the pumping power density of the laser adjusts the population of the energy levels and can cause a diverse set of possible emission wavelengths.²⁸

The spin forbidden 4f-4f transition, due to quantum mechanical selection rules, is relaxed due to local crystal-field inducing mixing of the f states with higher electronic configurations.²⁹ The primary forbidden nature of the f-f transition causes the lifetime luminescence to be long (up to tens of milliseconds), which favours sequential excitations in the excited state in the ESA process and also allows for favourable ion-ion interactions in the excited state states for permitting energy transfers between two or more Ln^{3+} ions in the ETU process, it also makes time-resolved luminescence techniques possible because of minimization of background fluorescence.^{8,11}

The sequential absorption of multiple photons through the use of real ladder-like intermediate energy levels, with long lifetime, provides a large anti-stokes shift, which allows for easy separation of the emission wavelength from the excitation wavelength.⁸ The narrow absorption profile limits the amount of possible excitation sources. However, the inexpensive InGaAs diode laser excites at 980 nm and matches well

with the absorption spectrum of the lanthanide-doped UCNPs. Since the upconverted emission is based on existing intermediate energy levels, it can be induced by a low power laser. Because the excitation is in the NIR region, which is within the optical transparency region, UCNPs allow for much deeper penetration depth and reduce the photodamaging of the tissue. In addition, this optical transparency window provides much higher signal-to-background ratio due to the absence of autofluorescence and reduced light scattering, compared to conventional biolabels.⁹

Since the upconverted emission from the 4f-4f transitions of Ln^{3+} does not involve chemical bond breaking, the UCNPs are stable against photobleaching and photochemical degradation, which implies that the UCNPs remain unaltered after irradiation by NIR lasers for hours.^{8,31} Furthermore, UCNPs, which usually contain many lanthanide dopants ions, possess non-blinking emission under a NIR excitation source.³¹

iii. Quantum yield

An import parameter that describes the emission efficiency of the UCNPs is defined as the quantum yield (QY) (equation 1). The nonlinear nature of the UC process indicates that the efficiency of this process is strongly dependent on the excitation power density. High efficiencies are required for biomedical applications to improve the limit of detection, to obtain higher signal-to-background ratio for bioimaging and for increased therapy effects.

$$\text{QY} = \frac{\text{number of emitted photons}}{\text{number of absorbed photons}} \quad (1)$$

Unfortunately, the QY in most UCNPs barely exceeds 1%. Currently, the highest reported QY developed by Huang *et al.*, is 7.6% for $\text{LiLuF}_4:\text{Yb}^{3+}/\text{Tm}^{3+}@\text{LiLuF}_4$

Table 1: Typical synthetic methods for lanthanide-based UCNPs.¹²

Synthetic method	Examples of hosts	Size range/nm	Advantages	Disadvantages
Co-precipitation	LaF ₃ , NaYF ₄	40-500	Narrow size distribution and tunable size, procedure are facile and time-saving, and no need for costly apparatus	Calcination or annealing is required
Thermal decomposition	Dy ₂ O ₃ , Y ₂ O ₃ , NaLnF ₄	3-150	High quality, narrow size distribution and highly monodispersed nanoparticles	Expensive and air-sensitive metal precursors, hydrophobic due to the passivating ligands frequently used, and toxic byproducts
Hydrothermal, solvothermal, liquid-solid-solution, ionic liquid synthesis	(La-Dy)VO ₄ , NaYF ₄ , YVO ₄	10-1000	Highly crystalline nanoparticles at lower temperature, cheap raw materials and simple procedures, and tunable crystal size and morphology	Specialized reaction vessels are required
Sol-gel processing	GdVO ₄	30-600	Cheap and raw materials and simple procedures	Broad particle size distribution and severely agglomerated, a heat treatment is usually required, and not suitable for bioapplication
Combustion synthesis	Gd ₂ O ₃	30-150	Time and energy saving, simple procedures	Severely agglomerated, broad particle size distribution
Flame synthesis	La ₂ O ₃ , Y ₂ O ₃	30-1000	Timesaving and simple procedures	Severely agglomerated, broad particle size distribution

core-shell nanocomplexes.³² In section 6, the disadvantages of low QY will be explained and new ideas are discussed.

IV. SYNTHESIS, SURFACE MODIFICATION AND BIOCONJUGATION OF UPCONVERSION NANOPARTICLES

To make use of the optical properties of UCNPs, their synthesis should be exploited such that pure nanoparticles with sufficient efficiency are obtained. In addition, the nanoparticles should be water soluble and non toxic for use in bio applications. To reach sufficient targeting and circulation, biomolecules can be attached to the surface of the nanoparticles.

i. Synthesis

To date, a diverse range of synthetic routes is entrenched for the composition, morphology and particle size of UCNPs.^{19,33} Many approaches for preparation techniques have been reported in literature. Zhang *et al*, reviewed the advantages and disadvantages of the typical synthetic methods for lanthanide-based UCNPs, which are shown in table 1.¹² The most used synthesis for pure UCNPs with

good morphology and efficient luminescence are co-precipitation, hydrothermal/solvothermal methods and thermal decomposition.¹² Combustion synthesis and flame synthesis are not so often used for UCNPs for biomedical applications as those particles suffer from agglomeration.¹²

ii. Surface modification

For the use of nanoparticles in biomedical applications, the nanocomplexes should be water soluble, without being cytotoxic. Because most methods for preparing good quality UCNPs involve the use of oleic acids, hydrophilic functional groups are required for providing water solubility. Functional groups are also used to make them biocompatible and to provide reactive groups for subsequent bioconjugation.

Using the ligand exchange strategy, one can replace the oleic acid by an active hydrophilic ligand such as polyethylene glycol (PEG), polyethylenimine (PEI), polyvinylpyrrolidone (PVP) and many more.³⁴⁻³⁶ UCNPs can also be covered with a amphiphilic copolymer via ligand attraction. The ligand oxidation strategy uses a strong oxidant to convert the carbon-carbon double bond of oleic acid into a hydrophilic carboxylic group. Another well-established method for surface modification is surface silanization, as it has good biocompatibility.

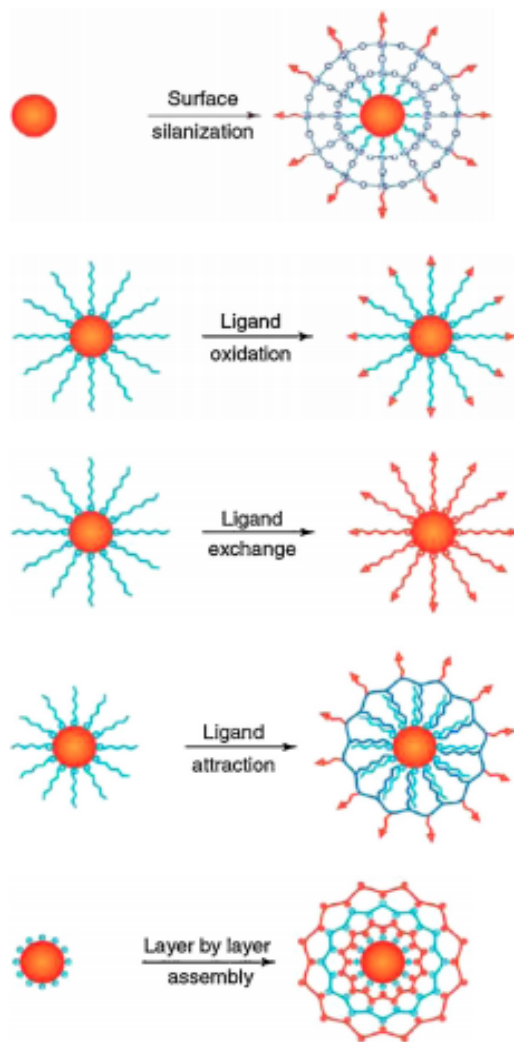


Figure 4: Typical strategies for the surface modification of lanthanide-doped UCNPs.¹²

ity. Additional chemical groups are easily introduced and there can be encapsulation of both hydrophilic and hydrophobic nanocomplexes. Furthermore, layer-by-layer assembly, which is based on the electrostatic attraction between oppositely charged polymers, make UCNPs water soluble. The different approaches for surface modifications are depicted in figure 4.

iii. Bioconjugation

So far, the surface modifications are limited to the surface nanochemistry that enables the particles to be stable and dispersible in aqueous solutions. However bioconjugation of nanoparticles with various functional biomolecules, such as antibodies, enzymes and DNA, can be attached to the nanoparticles for enhanced circulation and targeting, which is generally required for theranostic applications. There are several methods for the linking of biomolecules with nanoparticles. Because physical absorption on the surface is quite unstable and

has low loading capability, one preferably uses covalent conjugation. Commonly used functional groups such as $-\text{COOH}$, $-\text{OH}$, $-\text{SH}$ and $-\text{NH}_2$ can be covalently bound to the surface of the nanoparticles.¹²

V. UPCONVERSION NANOPARTICLES FOR BIOMEDICAL APPLICATIONS

Over the past decades, the tremendous amount of efforts in the synthesis, surface modification and bioconjugation of upconversion nanocrystals have led to big progress, especially in the realm of bioapplications such as imaging, sensing, drug delivery and therapy.

i. Drug delivery

In this section, the incorporation of lanthanide-doped UCNPs into light-initiated drug delivery systems is reviewed. The nanoparticles can be used as the up-converted light source to trigger drug release by photodegradation of photosensitive moieties. In addition, they can be used for fluorescence tracking and efficiency measurements of drug release.

In general, there are three approaches for the use of UCNPs for drug delivery, which are shown in figure 5. The first approach uses hydrophobic pockets where the drug is encapsulated into. This is done by making use of the hydrophobic surface of the UCNP which interacts with hydrophobic drugs. The second method deposits drugs in the pores of mesoporous silica shells, which are coated onto the UCNP surface, and the third method loads the drugs in hollow spheres coated with a mesoporous lanthanide shell.¹¹

So, in the first approach, there is an attraction between the hydrophobic ligands on the outer layer of the UCNP with the hydrophobic segment of an amphiphilic polymer due to van der Waals forces. As a consequence, the UCNP is now soluble in water. As mentioned before, a frequently used amphiphilic polymer is polyethylene glycol (PEG).³⁷ In the design of Wang *et al.*, the $\text{NaYF}_4:\text{Yb}^{3+}/\text{Er}^{3+}$ UCNP, capped with oleic acid, is encapsulated by PEGylated polymers, creating hydrophobic pockets on the surface.³⁷ The deprotonated lipophilic anticancer drug doxorubicin (DOX) can then be adsorbed into the hydrophobic pocket by hydrophobic interactions. The drug releasing profile was tested at neutral and acidic pH by incubating the drug loaded nanoparticles in phosphate buffer solution (PBS) at pH 7.4 and 5.0. In PBS at pH 7.4, about 20% of the DOX was released, whereas the amount of released DOX increased to 50% at pH 5.0 within 2 hours. Protonation of the amino group in the DOX offers the DOX a positive charge, which weakens its binding to the hydrophobic pockets and thus triggers the drug release.³⁷ It may be possible to have targeted drug delivery by conjugation of the end of the PEG chains with

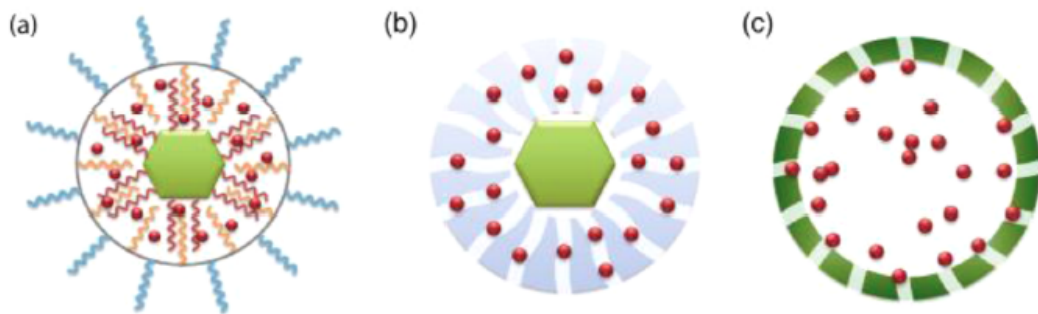


Figure 5: Schematic representation of different approaches to construct UCNPs for drug delivery systems: (a) hydrophobic pockets, (b) mesoporous silica shells, (c) hollow mesoporous-coated spheres.¹¹

targeting ligands like a folate acid. This increase in release with decreasing pH was a very favourable result for controlled drug release in tumor cells, as the pH in tumor cells is lower. Following up on this study, in 2014, Zhao's group proposed a highly efficient multifunctional nanoplatform for dual-modal luminescence imaging and pH-responsive drug delivery.³⁸ They covalently bind $\text{NaYF}_4:\text{Yb}^{3+}/\text{Er}^{3+}$ with downconversion fluorescent quantum dots. The obtained nanocomplexes can emit yellow fluorescence (downconversion process via quantum dots) and green luminescence (upconversion process via UCNPs) via irradiation with UV (365 nm) and NIR (980 nm) light, respectively. Enriched carboxylic groups in the polymer shell of the UCNPs make the nanocomposites soluble in water, functionalizable and provide the ability to load DOX by simple physical adsorption. Again, *in vitro* release of DOX was observed by changing the pH values. In neutral PBS, to simulate normal conditions, the release of the DOX was only 15.4% within 60 hours. In PBS of pH 5.0, to simulate the intracellular conditions of cancer cells, the release rate of the DOX reached about 69.5% within 60 hours. This favourable result provides a valuable method for the fabrication of functionalized UCNPs for dual-modal luminescence imaging and targeted cancer therapy. However, irradiation with 365 nm limits the penetration depth and can cause tissue burning very easily.

As mentioned earlier, another method to control drug release is silica coating. It is one of the most common techniques for surface engineering as silica exhibits low cytotoxicity and great chemical stability. In addition, it is possible to functionalize the pore system of the external particle surface and the porous structure provides a large surface area for drugloading.³⁹ Nevertheless, integration of UCNPs with a mesoporous silica coating usually requires complex synthesis and post-processing treatments.¹² In 2015, Li *et al.*, reported asymmetric single-hole mesoporous silica nanocages which can be endowed UC luminescence.⁴⁰ Bovine serum albumin protein can be stored at the outer surface of the UCNP and DOX can be accommodated in

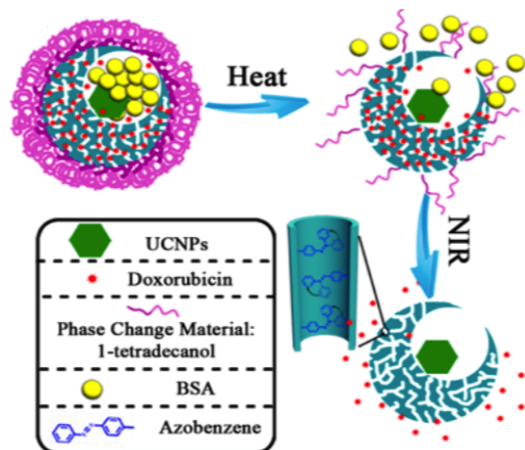


Figure 6: Scheme for controlled release of dual-sized guests by using the single-hole nanorattles modified with heat sensitive phase change materials and light sensitive molecules.⁴⁰

the mesoporous shell channels. As shown in figure 6, the single-hole nanorattles were modified with light sensitive azobenzene molecules in the mesoporous shell channels, and with heat sensitive phase change materials (1-tetradecanol) on the surface of the nanoparticles. It is a very interesting work since both small molecules and large guests can be stored in the particles. The bioactive compounds can be released by heat and NIR radiation independently with the assistance of the NIR to UV optical property of the UCNPs and the heat-sensitive phase change materials.⁴⁰ The discovery of the single-hole mesoporous nanocages may lead to the development of new architectures and concepts of nanoparticles for more multi-drug delivery systems and independent release.

A rather straightforward method for drug delivery is loading the drug into a hollow sphere, which is coated with a mesoporous lanthanide shell. In 2011, Lin's research group reported an Er^{3+} doped $\text{Yb}(\text{OH})\text{CO}_3@\text{YbPO}_4$ core-shell hollow spheres that exhibit strong green emission at 980 nm excitation.⁴¹ The group states that the DOX-loaded spheres exhibit greater cytotoxicity than free DOX, implying that is has

the potential to be used for drug loading and delivery for inducing cancer cell death. In this context, Lu *et al.* employed a novel UC luminescent nanorattle by incorporation of lanthanide-doped fluorides into hollow mesoporous silica.⁴² The nanorattles have high capacity due to hydrophobic interactions between the UCNPs and DOX. And again, the DOX showed fast release in pH 7.4, compared to the PBS solution of pH 5.0, caused by the enhanced electrostatic repulsion between DOX and the aminopropyl group of the mesoporous silica as well as by the repulsion between the DOX molecules. Therefore, these systems can be used as smart carriers for drug release by varying the pH from 7.4 to an acidic environment owing to endocytosis.

i *In vitro* and *in vivo* photoactivation

UV irradiation-mediated photochemical reactions are of importance for drug delivery systems. The UV photons have the ability to manipulate functions of biomolecules and can mediate on-demand drug release via photoactivation. Nevertheless, UV lasers and lamps have many drawbacks such as phototoxicity, a large radiation area and limited penetration depth. NIR-to-UV Ln³⁺-doped UCNPs can play a vital role in drug release mechanisms because of their deep penetration depth and ability to precisely light control drug release, as described in section 3.2 and 5.1. In addition, the radiation area is minimized to the nanometer regime.¹¹ For example, a direction for *in vitro* and *in vivo* photoactivation is NIR light-induced photoswitching of molecular switches to switch back and forth between different isomers. Capobianco and coworkers invented a NIR light photoswitching method by grafting bis-spiropyran onto the surface of LiYF₄:Yb³⁺/Tm³⁺ UCNPs via ligand exchange.⁴³ The UCNPs are excited at 980 nm and fluorescence resonance energy transfer from the UCNPs to the bis-spiropyran molecules on the surface can trigger the transformation of the ring-closed bis-spiropyran form to the ring-open bis-merocyanine form, which was achieved by irradiation at 365 nm. The reverse photocyclization can be achieved by radiation with visible light with a wavelength larger than 500 nm. The switched absorption peak may also be utilized for the manipulation of the color emission of the UCNPs inside the cell by changing the irradiation wavelength.

ii. Phototherapy

The impressive array of surface characteristics of lanthanide-doped UCNPs made them not only useful as vehicles for drug delivery and release but also for therapeutics. In this section, the different forms of therapy involving lanthanide-doped UCNPs are discussed. Phototherapies like photodynamic therapy (PDT) and photothermal therapy (PTT) garnered tremendous interest over the last years within biomedical applications.

i Photodynamic therapy

PDT involves the selective uptake and localization of a photosensitizer into specific tumor cells and tissue types. The photosensitizers can be activated by irradiation of a predetermined dose of light and can generate the cytotoxic reactive oxygen species (ROS), ¹O₂, which can kill cancer cells without affecting the surrounding tissue (see figure 7).^{44,45} The penetration depth of PDT is, however, only about one centimeter, which implies that only tumors just below the skin can be treated with PDT. Also destroying large tumors is very difficult with PDT. Currently, PDT is used for the treatment of prostate, lung, neck, head, and skin cancers.⁴⁶

The explained deep penetration depth of UCNPs caused large interest in using them for cancer therapy. The emitted light from the UCNPs can excite photosensitizers, which then generate the ROS, in order to destroy the tumor cells, and drawbacks of existing PDT can be overcome. This idea was firstly proposed by Prasad *et al.*, and was realized by Zhang *et al.*^{47,48} They encapsulated merocyanine 540 as photosensitizer into a silica layer which was coated on Y₂O₃:Yb³⁺/Er³⁺ UCNPs. An antibody, specific to antigens on the target cell surface, was covalently attached to the UCNPs. Irradiation with NIR leads to the upconverted emission, which is then absorbed by the photosensitizers. Subsequently, excited photosensitizers interact with ground-state molecular oxygen, and generate ROS, which eventually leads to cancer cell death *in vitro*.

Liu and coworkers reported the pioneering work to show the effectiveness of upconversion for *in vivo* PDT.⁴⁹ They used the porphyrin derivative chlorine 6 (Ce6) as photosensitizer which was non covalently incorporated into PEGylated coated β-NaYF₄:Yb³⁺/Er³⁺. The direct injection of the photosensitized UCNPs into the tumor showed 70% tumor regression after 30 minutes under 980 nm light irradiation. The tissue penetration abilities between UCNP-based PDT and traditional PDT in pork tissue was tested. Direct exposure of Ce6 solution with 660 nm excitation source generated much more ROS compared to the generation of ROS in UCNPs sensitized with Ce6, which was exposed with a 980 nm excitation source. However, ROS formation was completely eliminated when the 660 nm light was blocked by a 8 mm tissue, implying that the penetration depth is much deeper for UCNP-Ce6 nanocomplexes, because for those nanocomplexes, only 50% of the light was blocked by 8 mm pork tissue and still ROS was generated. The selectivity of the UCNP-Ce6 into tumor sites was not reported here, which is important for *in vivo* photodynamic therapy. Modification of active targeting ligands to the UCNPs is required for the increase of local concentration in tumors and to avoid side effects, and even if there is no control of where the UCNPs go, they should only be activated where needed.

In 2012, Zhang and coworkers reported a novel

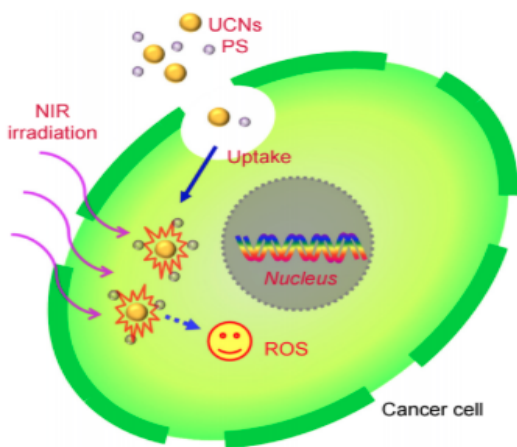


Figure 7: Schematic illustration of the UCNPs-based PDT treatment.⁵⁰

way to amplify therapeutic effects by the multicolor-emission capability of UCNPs at a single 980 nm excitation wavelength for the simultaneous activation of two sensitizers.⁵³ They prepared the NaYF₄ UCNPs by uniformly coating them with mesoporous silica (figure 8a). The multicolor-emission capability of the UCNPs was used to activate two photosensitizers. The two emissions, green and red, from the UCNPs matched well with the absorption of the photosensitizers, merocyanine 540 (MC540) and zinc(II)phthalocyanine (ZnPc), respectively (figure 8b). The dual-photosensitizer approach was used as it showed enhanced generation of ROS and reduced cell viability. They first irradiated B16-F0 cells labeled with each of the differentially loaded UCNPs under the skin of mice. Irradiation by a 980 nm laser showed an increase in ROS, and the green fluorescence intensity was more intense than that of cells treated with either of the sensitizers. Secondly, they showed the efficacy of the UCNPs *in vivo* in mice. They intratumorally injected coloaded UCNPs into B16-F0 cells in mice and shined on the tumor with the NIR laser. As controls, other mice received intratumoral injection of PBS (the vehicle in which the UCNPs were suspended). The growth of the tumor cells with injected coloaded UCNPs was significantly inhibited (figure 8c and figure 8d). Extension of the study showed targeted PDT efficacy of folic acid (FA) conjugated PEGylated UCNPs (figure 8e). The B16-F0 tumors in mice where injected intravenously with coloaded FA-PEG-UCNPs and irradiated with a 980 nm laser. The tumor growth was reduced compared to the mice treated with PBS (figure 8f). The photosensitizers may be prematurely released from the nanoparticles, which can cause a reduction in efficiency of the cancer treatment, as they are solely physically entrapped inside the mesoporous silica. If they would be covalently bound at the surface of the nanoparticles, the premature release may be overcome.

Very recently, Lin and coworkers designed a core-shell structured NaGdF₄:Yb³⁺/Tm³⁺@NaGdF₄:Yb³⁺@NaNdF₄:Yb³⁺@NaGdF₄@mSiO₂@TiO₂ nanocomplex by coating a layer of TiO₂ photosensitizer on an effective 808 nm upconversion luminescent core to achieve simultaneous bioimaging and efficient PDT.⁵⁴ Thus far, most reported light-controlled therapies are based on NIR light excitation. This wavelength can directly overlap with the water absorption spectrum and can thus cause tissue heating (see section 6.2). The excitation wavelength of 880 nm has much less overlap with the absorption spectrum of water and therefore greatly minimizes heating of the tissue. The constructed design limits the reverse energy transfer from activator to sensitizer and thus improves the UC emission efficiency. The high surface area of the silica coated nanoparticle makes it very stable and enables high loading possibilities. *In vivo* results indicate much higher efficacy due to deeper penetration depth when exciting with a high wavelength. The nanocomplex itself can simultaneously be used as an imaging probe. For nanoplatforms with multifunctional properties for simultaneous therapy and imaging, the design should take into account that the absorption of the photosensitizer should have minimal mismatch with the upconverted emission to possess high UC efficiency and thus larger ROS production.

In addition to cancer therapy, UCNPs for photodynamic therapy have been extended to the reduction of viral infections, which provides promising antiviral approaches for treatment of viral infections.¹¹ PEI-NaYF₄:Yb³⁺/Er³⁺ loaded with a ZnPc photosensitizer was used for intra and extracellular inactivation of adenoviruses and dengue viruses as a consequence of the production of ROS.⁵⁵ Reduction in the infectious virus *in vitro* was shown in a murine model under NIR excitation source. The conjugation of antibodies or enzymes on the UCNPs provide the ability to specifically localize the UCNPs to the virus-infected cells only. It is quite an unexplored area, but yet shows potential for nanomedicine.

ii Photothermal therapy

The basic principle of photothermal therapy (PTT) is that normal cells and tumor cells have different sensitivity to heat. Healthy cells are more resistant to heat and have faster recovery when exposed to heat or radiation. Under NIR radiation, photothermal agents can convert light into heat to induce hyperthermia (higher than 42 °C) resulting in thermal ablation of the tumor cells, with minimal effect on the normal cells.⁵⁶ In order for effective cell death of tumor cells, the photothermal agent should have a high absorption coefficient to NIR radiation, well-engineered surface modifications and good biodegradability to dodge toxicity effects.⁵⁷ For an

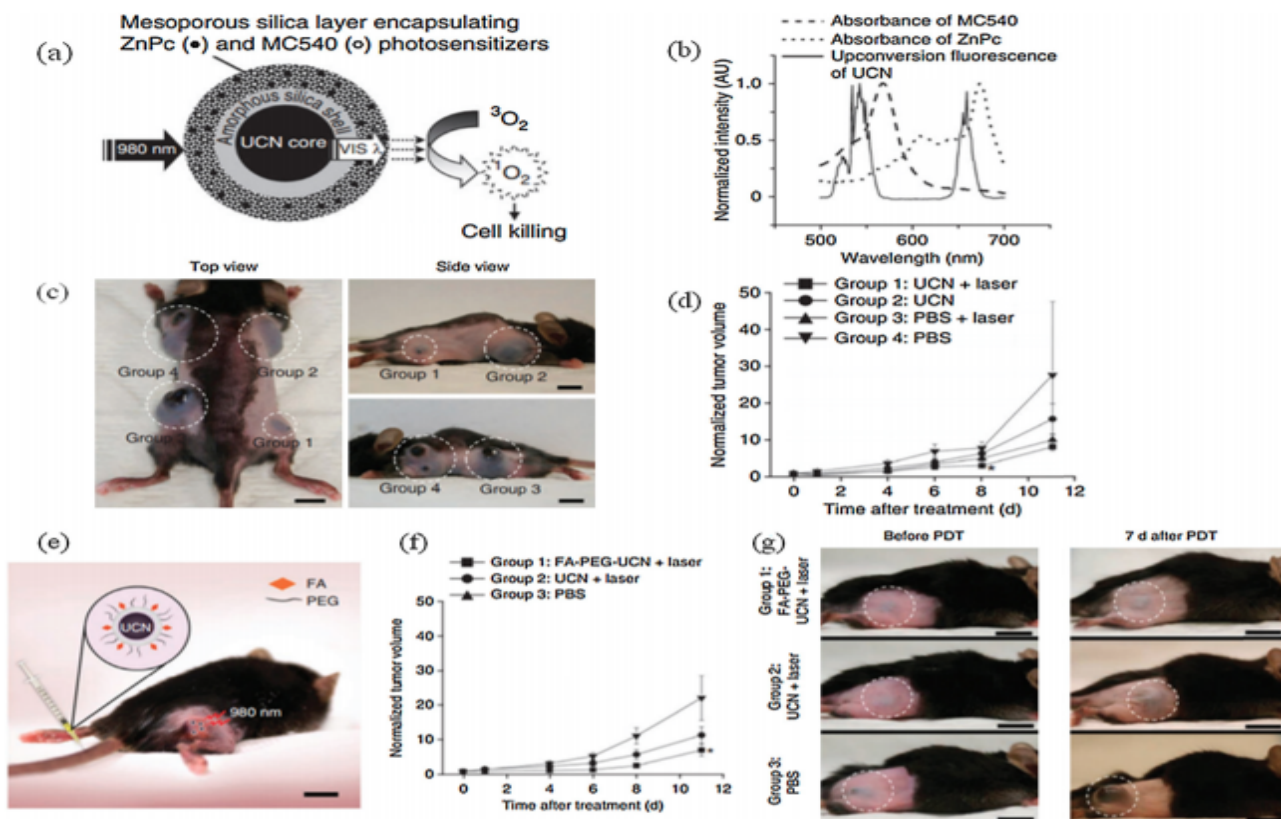


Figure 8: (a) Schematic of mesoporous-silica-coated $\text{NYF}_4:\text{Yb}^{3+}/\text{Er}^{3+}$ coloaded with ZnPc and MC540 for PDT. (b) The fluorescence emission spectrum of the UCNPs under 980-nm NIR laser excitation and the absorption spectra of ZnPc and MC540. (c) Photos of a mouse showing tumors at 14 days after treatment with the conditions described for groups 1-4. (d) Tumor volumes in the four treatment groups at 6, 8, 10, 12 and 14 days after treatment to determine the effectiveness of the treatment in terms of tumor cell growth inhibition. (e) Diagram showing UCNP-based targeted PDT in a mouse model of melanoma intravenously injected with UCNPs surface modified with FA and PEG moieties. (f) Change in tumor size as a function of time after treatment to assess the effectiveness of UCNP-based mediated targeted PDT in tumor-bearing mice intravenously injected with FA-PEG-UCNPs. (g) Photos of a mouse from each group 1-3 intravenously injected with FA-PEG-UCNPs, unmodified UCNPs or PBS showing the change in tumor size before and 7 days after PDT treatment.¹²

accurate and comprehensive assessment of the therapy results, as well as the visualization of the photothermal agent internalization and the size and location of the tumors, a multifunctional nanoplatform, consisting of several functional nanostructures in a hybrid system should be constructed. This nanoplatform can satisfy requirements for simultaneous therapy and diagnosis under imaging guidance. A possible manner to reach this is by combining the photothermal agents with lanthanide-doped UCNPs.⁵⁷ There exist different photothermal agents to combine with UCNPs to convert heat for inducing hyperthermia, such as gold-based nanoplatforms like nanorods and nanoshells, carbon-based materials such as graphene oxide and carbon dots, metal chalcogenides and organic molecules or polymers.⁵⁷

Very high temperatures kill not only cancer cells, but also damage the surrounding healthy tissue, resulting in side effects and influencing the precision of the photothermal therapy. Therefore, Zhy *et al.* built a carbon-coated core-shell upconversion

nanocomplex $\text{NaLuF}_4:\text{Yb}^{3+}/\text{Er}^{3+}@\text{NaLuF}_4@\text{Carbon}$ (core-shellUCNP@C) to real-time monitor the fluctuations in temperature in PTT.⁵¹ They made it possible to measure the difference between the apparent temperature (overall temperature of the lesion) and the eigen temperature (temperature of the nanoparticle). In addition, they used the nanocomplex as a temperature-feedback system to determine the dose of irradiation for PTT. Figure 9 is a schematic of the temperature-feedback core-shellUCNP@C used for accurate PTT at a facile temperature. The change in temperature of the carbon shell (which is the photon absorber) under 730 nm irradiation was monitored with temperature sensitive emission from the core-shellUCNP. They showed that the temperature of the nanoparticle was much higher than the temperature of the overall lesion, implying that the microscopic temperature of the photothermal material upon illumination is enough to kill cancer cells while the temperature of the lesions is still low enough to prevent the normal tissue from being damaged. Nevertheless, they used two

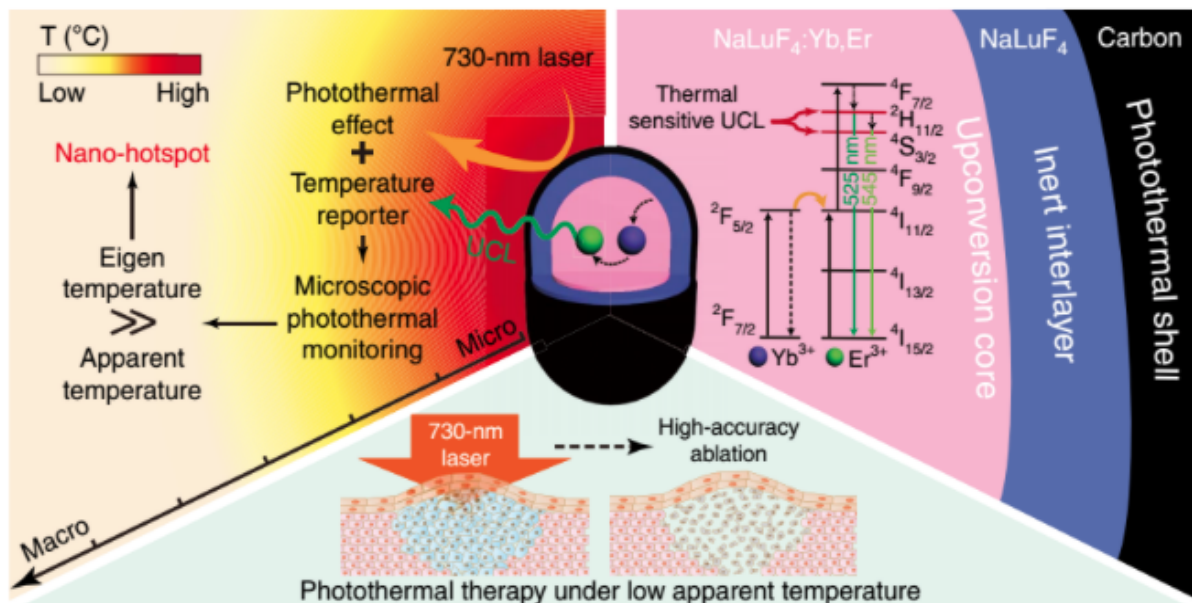


Figure 9: Schematic illustration of core-shell UCNP@C for accurate PTT at facile temperature. The core-shell UCNP@C exhibit both UCL emission and photothermal effect. With temperature-sensitive upconversion emission, core-shell UCNP@C was used to monitor the change in microscopic temperature of the photoabsorber (carbon shell) under 730 nm irradiation. The eigen temperature of the core-shell UCNP@C was much higher than the apparent temperature observed macroscopically, indicating that core-shell UCNP@C acted as a nano-hotspot at the microscopic level. By utilizing the high eigen temperature during photothermal process, accurate PTT, which prevent the damage to normal tissue can be realized.⁵¹

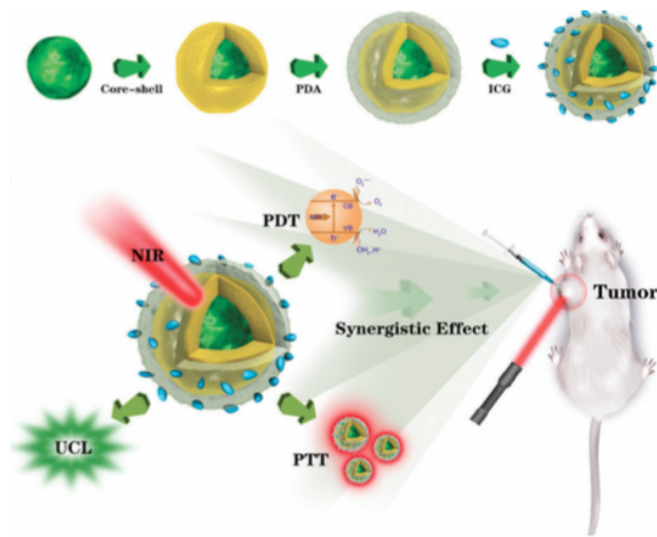


Figure 10: Schematic illustration for the synthetic procedure of UCNP@PDA-ICG nanocomposites and a schematic illustration of UCNP@PDA-ICG nanocomposites for upconversion imaging and synergistic PDT/PTT.⁵²

different laser wavelengths, 730 nm and 980 nm, for simultaneous excitation of the luminescence and the heat production. This complicates the experimental set up and creates an uncertainty in the thermal reading because of unequal penetration depths of the excitation wavelengths.

Other work is performed on building nanoplatforms for UC luminescence assisted PTT and PDT, which show

great promise in the detection and treatment of tumors. Very recently, Lin and coworkers developed polydopamine (PDA)-shelled $\text{NaYF}_4:\text{Yb}^{3+}/\text{Er}^{3+}$ UCNPs (UCNPs@PDA-ICG), as shown in figure 10, which are capable of loading indocyanine green (ICG) via electrostatic adsorption, hydrophobic interaction and $\pi - \pi$ stacking for UC imaging and combined PTT and PDT.⁵² The ICG drug can be triggered by 808 nm irradiation to produce the photothermal effect and the cytotoxic ROS simultaneously. Meanwhile, the PDA-coated UCNPs were used for UC emission imaging (figure 10). It was found that the growth of the tumors greatly inhibited after PDT/PTT combined therapy after 13 days post treatment. They state that *in vivo* and *in vitro* biocompatibility and bio-distribution experiments showed no obvious toxicity effects of the nanocomplexes. However, they did toxicity measurement for only seven days.

iii. Lanthanide nanocomplexes in other therapy forms

UCNPs are not only used for PTT and PDT but may also provide help for improving other therapeutic approaches. Radiation therapy is widely used for cancer therapy, and uses high-energy radiation, like an x-ray source, to reduce the tumor size and to kill cancer cells. Nevertheless, the normal tissue is also damaged by radiation therapy. Therefore, it is essential to develop a strategy that lowers the irradiation burden, and increases the efficacy even, in tumors that are radio-resistant. In

2013, Shi and coworkers developed a rattle-structured multifunctional UC nanoparticle with a porous silica shell for the delivery of cisplatin to tumors for chemo-/radiotherapy by cisplatin radiosensitization and luminescent/magnetic dual-modal imaging.⁵⁸ They showed that, *in vitro*, the UCNPs loaded with cisplatin were much more effective as radiosensitizer than free cisplatin. *In vivo* studies demonstrated enhanced radiotherapy efficiency of the drug loaded UCNPs and achieved simultaneous imaging and therapy via synergistic chemo-/radiotherapy.

Although radiative therapy is widely accepted for cancer treatment, it can cause damage to healthy cells which are close to cancer cells, due to the production of ROS during treatment processes. Antioxidant therapy is a general term for the use of any agent to reduce ROS. Cerium oxide nanoparticles (nanoceria) is finding widespread use in the treatment of medical disorders caused by the reactive oxygen intermediates, as it can switch between Ce(III) and Ce(IV) based on the environment.⁵⁹

UCNPs can also be used for gene therapy, which is the therapeutic delivery of nucleic acids into targeted cells to correct for defective genes. Ln^{3+} nanocomplexes were introduced as non viral systems to deliver genes into the targeted cells, to overcome toxicity problems and immunological and inflammatory limitations.⁶⁰ As an example, Zhang and coworkers reported exploitation of $\text{NaYF}_4:\text{Yb}^{3+}/\text{Tm}^{3+}$ UCNPs functionalized with a mesoporous silica shell.⁶¹ DNA/siRNA was photocaged by 4,5-dimethoxy-2-nitroacetophenone (DMNPE) and loaded into the shell. The mesoporous shell enabled delivery of high payload and protection of the nucleic acids from the environment. The upconverted UV emission from the UCNPs behaves as a switch to uncage the nucleic acids, thereby rendering it fully functional for exerting its effect in the host cells.

VI. REMAINING CHALLENGES FOR LANTHANIDE-DOPED UPCONVERSION NANOPARTICLES

This review has surveyed the recent advancements in the design, synthesis and chemistry of UCNPs, as well as their applications in drug delivery and therapy. Despite the rapid development of UCNPs due to their, previously described, unique optical and chemical properties such as the large Stokes-shift, nonphotobleaching behaviour, no autofluorescence, low photodamage to cells, and deep penetration depth, there remain some shortcomings which hinder practical applications, and will be discussed in this section.

i. Quantum yield and extinction coefficient

While direct excitation in downconversion processes show a quantum yield of about 25%, the quantum yield of UC luminescence is often barely more than 1%, and reduces as the size of the UCNP decreases.⁶² This implies that high power excitation is required for the light responsive materials to work for probing deep tissue systems, as a low QY limits the brightness of the UCNPs. A high QY is also required for PDT applications in order to produce enough ROS for killing cancer cells. Finding new activator/emitter combinations and tuning their concentrations, as well as new possibilities for surface manipulation may further help for enhancing emission, tissue penetration depth and QY. Other novel ways for QY improvements may be reached by the development of UCNPs with a suitable crystal field symmetry, increased particle size, and a low phonon energy host, as explained in section 3.2. Core-shell structures that spatially isolate the Ln^{3+} ions in the core from the shell can upgrade the QY by preventing cross relaxations, which often limit the efficiency. The coupling of UCNPs to other emitters via fluorescence resonance energy transfer (FRET) and luminescence resonance energy transfer (LRET) can open new possibilities for higher QY.^{11,63} Additionally, plasmon resonances can enhance the emission rate.⁶⁴ The goal of the plasmon-enhanced UC is to improve the absorption and emission processes by tailoring the magnetic and electric field at the UCNPs, by adopting the high-frequency electromagnetic resonances of electrons in conducting elements. In FRET, the upconverted emission from the donor fluorophore is nonradiatively transferred to the acceptor fluorophore via dipole-dipole coupling.⁶⁵ The upconverted emission wavelength has a much larger freedom when the energy is transferred to, for example, an organic dye or a quantum dot acceptor, and a wide range of colors can be produced.⁶⁶ This result makes broadband UC possible, as practical applications are often limited by the narrowband NIR absorption. Hummelen and coworkers proposed that by using suitable co-sensitizing sets of organic dyes as antenna molecules and UCNPs, it will be possible to obtain broadband UC where light is absorbed in the full desired spectral range, as the absorption of the dyes is orders of magnitude larger than the absorption of Ln^{3+} ions.⁶⁷ This antenna effect can provide possibilities for engineering the excitation energy for UCNPs, which eliminates the necessary match between the excitation and the absorption of the Ln^{3+} ions. However, one can argue that it is preferred that specific applications of UCNPs occur at specific wavelengths only. Also the photobleaching may be succumb by such organic dyes, which makes them unsuitable for long-term activation and imaging applications. In LRET, the energy transfer process is radiative and studies showed effective expansion of the

UC luminescent emissions.⁶³

So, the prohibitively low efficiencies of current materials makes integration of UCNPs into biomedical applications difficult and development of UCNPs with higher QY is therefore considerably important.

ii. Toxicity and biodegradability

In addition, there exist a general concern of the effect of nanoparticles on health and environment. Predicting the potential toxicity is a significant challenge as the biotoxicity depends on many different factors like size, dosage, surface modifications and functionalization, material type, surface charge, cell types, cell incubation time, local chemical and physical environment, etc.^{10,11,68,69} This implies that nanotoxicology should take many more interdependent parameters into account than conventional toxicological studies, which solely focus on concentration, composition and exposure time. In order to understand the toxicity of the Ln³⁺-doped UCNPs, the chemical characterisation of the UCNPs and their reactivity when the surface is in contact with living cells should be known.

The majority of *in vitro* studies have shown that lanthanide-doped UCNPs are tested to have negligible or low toxicity in a certain concentration range and for a limited incubation period, implying that their applications remain undoubtedly highly promising and competitive to traditional approaches.^{11,12,69} Although the chemical elements of lanthanide-doped UCNPs may be non-toxic, and secondary toxicity effects through interactions of degradation products with the cellular biochemical environment are not observed, the chemical and physical properties of the nanocomplexes as a whole may cause various effects.⁶⁹ Also, extensive research should be performed to test the long-term (i.e. a few animal generation) toxicity effects of the UCNPs and the reagents and ligands used in the synthesis, on and with the immune system, possible interference with the reproductive system and affection of the next generation, before going into clinical use.⁷⁰ In addition, the use of UCNPs for *in vivo* applications is questionable. This is mostly due to the lack of knowledge considering primary and secondary toxicity effects of the nanoparticles on the human body and the environment.

Another need is the understanding of where and how nanoparticles accumulate in the body, and what time is indispensable to get the nanoparticles from the different organs, like liver, lungs and spleen. Nowadays, most nanoparticles accumulate in reticuloendothelial systems, such as the liver and spleen.⁶⁸ For improvements of pharmacokinetics, tumor targeting and toxicity, there is need for the optimization of the surface coating and the size of UCNPs, as well as for directed diffusion and incorporation of selective and precise targets on the cellular level. Nanocomplexes usually do

not degrade into biological compounds, and therefore, may contribute to secondary toxicity effects. In order for the nanoparticles to degrade, cells have to contain enzymes which are capable of breaking the bonds of the nanomaterials, and in most cases, these enzymes are not existing in the cells. In order to efficiently excrete the nanoparticles via the urinary system, sub-10 nm particles should be prepared.⁷¹ Small nanoparticles are also much more efficient taken in by endocytosis. Reports show that nanocomplexes with a diameter larger than 20 nm are slowly excreted by the urinary system and can circulate in the body for longer than a week, which is sufficient for the UCNPs to interact with the biological environment and other nanoparticles and to cause toxic effects.^{69,72} Paradoxically, the objective for using nanoparticles is for facilitating diffusion and incorporation of very selective and precise targeting possibilities at the subcellular level.

As mentioned in section 5.1, the excitation wavelength of 980 nm overlaps with the absorption spectrum of water, causing undesirable tissue heating under NIR radiation. Using a shorter excitation wavelength can greatly minimize the tissue heating and investigations in core-shell structures or multiple sensitizers can cause a blue shift in the excitation wavelength.

Another issue for nanoparticles in the body is the nanoparticle-protein corona, which is a protein adsorption layer that forms on the surface of colloidal nanoparticles when they enter a biological fluid. Proteins are major constituents of biological fluids and generally adsorb on the surface of materials. The composition of the corona is dependent on both the particle and the protein. This corona can change the properties of the modified nanoparticles with bioactive molecules and capping agents. In order to prolong the stability of the nanoparticles and to reach longer circulation in the blood for *in vivo* targeted drug delivery, studies should be performed on surface engineering to avoid the adsorption of proteins on the material surface.

From many reviews and papers, it can be concluded that knowledge on the general impact of nanoparticles on human health is not well established. Even the most comprehensive EU chemical legislation, REACH, does not refer to nanoparticles in special. The current toxicity evaluations lack uniformity in the nanoparticle parameters, like chemical composition (of the nanoparticles itself), physical parameters (i.e. structure, size distribution, agglomeration, distribution), surface state (i.e. surface charge/porosity/functionality/hydrophilicity/lipophilicity/phobicity), local chemical and physical environmental factors (i.e. pH, temperature, protein-corona formation), presence of other chemicals/biocomponents or electromagnetic fields, etc. The knowledge of these parameters is indispensable for the understanding of the toxicity of the nanoparticles. The lack of standardized protocols for the assessment of

toxicity is a very important issue in the determination of the toxicity of nanoparticles for clinical trials, as it is difficult to compare results from various studies as they are measured under different conditions (time of exposure and dose) using particles with varying morphology, size, surface charge, chemical composition and functional groups.⁷² All in all, knowledge of the interactions with the body is paramount in order to know the potential effects that nanoparticles may have as nanotoxicological studies should take many more interdependent parameters into account than conventional studies on toxicity determination.

VII. SUMMARY AND FUTURE DIRECTIONS

I have endeavored to review the recent developments of lanthanide-doped upconversion nanoparticles, and to offer unique insights into their diverse and multipurpose applications in the field of drug delivery and therapy for nanomedicine. This review describes the fundamentals of the upconversion principles and the chemical aspects of lanthanide-doped UCNPs, as well as their synthesis, surface modification and bioconjugation strategies. The distinct properties of lanthanide-doped upconversion nanoparticles, like long-lived intermediate energy states, large anti-stokes shift, sharp emission peaks, high resistance to photobleaching, chemical degradation and photoblinking, deep penetration depth and absence of autofluorescence, have led to the rapid development of many bioapplications over the past few years. A wide set of promising demonstrations for biomedical applications like targeted drug delivery, photodynamic therapy, photothermal therapy, and other therapy forms, is reported and UCNPs have shown to be promising for this class of materials. Nevertheless, there remain some issues, which are addressed in section 6, before they can go into clinical use. One of the crucial issues is their low QY. New activator/emitter combinations in various concentrations and manipulation of the ligands on the particles may higher the QY, which is especially required for deep tissue imaging. Other concerns like biodegradation, biodistribution, long-term toxicity and stability and biocompatibility of nanoparticles in general, should be thoroughly evaluated for UCNPs to be used in biomedical applications. Current evaluations on toxicity lack uniformity in parameters of the nanocomplexes. In addition, it should be noted that Wilhelm *et al.*, did an analysis of nanoparticle delivery to tumours and found that only 0.7% (median) of the administered nanoparticle dose is found to be delivered to a solid tumour, whereas the remaining particles circulate in the body.⁷³

Years of development have brought the upconversion nanoparticles for biomedicine from cell level to different animals, with great advantages on diagnosis, drug delivery, therapy and imaging. However, most of

the demonstrated results have been obtained *in vitro* and more work should be performed to demonstrate the *in vivo* use of UCNPs. In addition, a higher payload and improved targeted release of drugs should be employed for the use of UCNPs in drug delivery. Also the apparatus for the optical characterization of the nanoparticles is laboratory customized, and most commercial instruments used in clinics are based on down-conversion probes.

Future applications in the exciting field of UCNPs require the synergistic efforts of multidisciplinary collaboration between scientists from material science and clinical medicine to further push forward the potential in clinical applications and to open new promises in nanomedicine for Ln³⁺-doped UCNPs. Studies should focus on the development of a general synthetic approach, which is easily reproducible for large scale, and contains multifunctional properties for simultaneous diagnosis, therapy and imaging, which can be of high potential for the inclusion of lanthanide-doped upconversion nanoparticles in biomedicine. It is envisioned that lanthanide-based UCNPs will continue to be ardently studied as one of the platforms for the evolution of biomedicine based on nanocomplexes.

VIII. ACKNOWLEDGEMENTS

I would like to thank my supervisor Dr. A. Salvati for the useful and extensive feedback she gave. I appreciate the fact that she was willing to invest time and effort in guiding me through the process of writing this review. I also thank Prof. A. Herrmann for being my second supervisor and Dr. M.S. Pshenichnikov, Prof. Dr. R.C. Chiechi and Prof. T. Banerjee for the useful lectures on paper writing and scientific integrity.

REFERENCES

1. Bloembergen, N. Solid state infrared quantum counters. *Physical Review Letters* **2**, 84 (1959).
2. Liu, X., Yan, C.-H. & Capobianco, J. A. Photon upconversion nanomaterials. *Chemical Society Reviews* **44**, 1299–1301 (2015).
3. Auzel, F. Upconversion and anti-stokes processes with f and d ions in solids. *Chemical reviews* **104**, 139–174 (2004).
4. Wang, F. & Liu, X. Upconversion multicolor fine-tuning: visible to near-infrared emission from lanthanide-doped NaYF₄ nanoparticles. *Journal of the American Chemical Society* **130**, 5642–5643 (2008).
5. Heer, S., Kömpe, K., Güdel, H.-U. & Haase, M. Highly efficient multicolour upconversion emission in transparent colloids of lanthanide-doped NaYF₄ nanocrystals. *Advanced Materials* **16**, 2102–2105 (2004).

6. Chatterjee, D. K. & Yong, Z. Upconverting nanoparticles as nanotransducers for photodynamic therapy in cancer cells. *Nanomedicine* **3**, 73–82 (2008).
7. Idris, N. M. *et al.* Tracking transplanted cells in live animal using upconversion fluorescent nanoparticles. *Biomaterials* **30**, 5104–5113 (2009).
8. Wang, F., Banerjee, D., Liu, Y., Chen, X. & Liu, X. Upconversion nanoparticles in biological labeling, imaging, and therapy. *Analyst* **135**, 1839–1854 (2010).
9. Liu, Y., Tu, D., Zhu, H. & Chen, X. Lanthanide-doped luminescent nanoprobe: controlled synthesis, optical spectroscopy, and bioapplications. *Chemical Society Reviews* **42**, 6924–6958 (2013).
10. Wang, M., Abbineni, G., Clevenger, A., Mao, C. & Xu, S. Upconversion nanoparticles: synthesis, surface modification and biological applications. *Nanomedicine: Nanotechnology, Biology and Medicine* **7**, 710–729 (2011).
11. Chen, G., Qiu, H., Prasad, P. N. & Chen, X. Upconversion nanoparticles: design, nanochemistry, and applications in theranostics. *Chemical reviews* **114**, 5161–5214 (2014).
12. Zhang, Y., Wei, W., Das, G. K. & Tan, T. T. Y. Engineering lanthanide-based materials for nanomedicine. *Journal of Photochemistry and Photobiology C: Photochemistry Reviews* **20**, 71–96 (2014).
13. Wang, F. *et al.* Tuning upconversion through energy migration in core–shell nanoparticles. *Nature Materials* **10**, 968–973 (2011).
14. Chivian, J. S., Case, W. & Eden, D. The photon avalanche: A new phenomenon in Pr³⁺-based infrared quantum counters. *Applied Physics Letters* **35**, 124–125 (1979).
15. Haase, M. & Schäfer, H. Upconverting nanoparticles. *Angewandte Chemie International Edition* **50**, 5808–5829 (2011).
16. Dong, H., Sun, L.-D. & Yan, C.-H. Basic understanding of the lanthanide related upconversion emissions. *Nanoscale* **5**, 5703–5714 (2013).
17. Dexter, D. L. A theory of sensitized luminescence in solids. *The Journal of Chemical Physics* **21**, 836–850 (1953).
18. Joubert, M.-F. Photon avalanche upconversion in rare earth laser materials. *Optical materials* **11**, 181–203 (1999).
19. Zhou, B., Shi, B., Jin, D. & Liu, X. Controlling upconversion nanocrystals for emerging applications. *Nature nanotechnology* **10**, 924–936 (2015).
20. Zhou, J., Liu, Q., Feng, W., Sun, Y. & Li, F. Upconversion luminescent materials: advances and applications. *Chemical reviews* **115**, 395–465 (2014).
21. Liu, Y. *et al.* A strategy to achieve efficient dual-mode luminescence of Eu³⁺ in lanthanides doped multifunctional NaGdF₄ nanocrystals. *Advanced Materials* **22**, 3266–3271 (2010).
22. Page, R. H. *et al.* Upconversion-pumped luminescence efficiency of rare-earth-doped hosts sensitized with trivalent ytterbium. *JOSA B* **15**, 996–1008 (1998).
23. Wang, M. *et al.* Two-phase solvothermal synthesis of rare-earth doped NaYF₄ upconversion fluorescent nanocrystals. *Materials Letters* **63**, 325–327 (2009).
24. Shan, S.-N., Wang, X.-Y. & Jia, N.-Q. Synthesis of NaYF₄: Yb³⁺, Er³⁺ upconversion nanoparticles in normal microemulsions. *Nanoscale research letters* **6**, 539 (2011).
25. Chen, G., Liu, H., Somesfalean, G., Liang, H. & Zhang, Z. Upconversion emission tuning from green to red in Yb³⁺/Ho³⁺-codoped NaYF₄ nanocrystals by tridoping with Ce³⁺ ions. *Nanotechnology* **20**, 385704 (2009).
26. Krämer, K. W. *et al.* Hexagonal sodium yttrium fluoride based green and blue emitting upconversion phosphors. *Chemistry of Materials* **16**, 1244–1251 (2004).
27. Zhang, C., Lingdong, S., Zhang, Y. & Chunhua, Y. Rare earth upconversion nanophosphors: synthesis, functionalization and application as biolabels and energy transfer donors. *Journal of Rare Earths* **28**, 807–819 (2010).
28. Xue, X. *et al.* Laser power density dependent energy transfer between Tm³⁺ and Tb³⁺: tunable upconversion emissions in NaYF₄: Tm³⁺, Tb³⁺, Yb³⁺ microcrystals. *Optics Express* **24**, 26307–26321 (2016).
29. Judd, B. Optical absorption intensities of rare-earth ions. *Physical Review* **127**, 750 (1962).
30. Wang, F. & Liu, X. Multicolor tuning of lanthanide-doped nanoparticles by single wavelength excitation. *Accounts of chemical research* **47**, 1378–1385 (2014).
31. Wu, S. *et al.* Non-blinking and photostable upconverted luminescence from single lanthanide-doped nanocrystals. *Proceedings of the National Academy of Sciences* **106**, 10917–10921 (2009).
32. Huang, P. *et al.* Lanthanide-Doped LiLuF₄ Upconversion Nanoprobes for the Detection of Disease Biomarkers. *Angewandte Chemie International Edition* **53**, 1252–1257 (2014).

33. Yang, Y., Velmurugan, B., Liu, X. & Xing, B. NIR photoresponsive crosslinked upconverting nanocarriers toward selective intracellular drug release. *Small* **9**, 2937–2944 (2013).
34. Jin, J. *et al.* Polymer-coated NaYF₄: Yb³⁺, Er³⁺ upconversion nanoparticles for charge-dependent cellular imaging. *ACS nano* **5**, 7838–7847 (2011).
35. Chien, Y.-H. *et al.* Near-infrared light photocontrolled targeting, bioimaging, and chemotherapy with caged upconversion nanoparticles in vitro and in vivo. *Acs Nano* **7**, 8516–8528 (2013).
36. Li, Z. & Zhang, Y. Monodisperse silica-coated polyvinylpyrrolidone/NaYF₄ nanocrystals with multicolor upconversion fluorescence emission. *Angewandte Chemie* **118**, 7896–7899 (2006).
37. Wang, C., Cheng, L. & Liu, Z. Drug delivery with upconversion nanoparticles for multi-functional targeted cancer cell imaging and therapy. *Biomaterials* **32**, 1110–1120 (2011).
38. Zhao, P. *et al.* A novel strategy for the aqueous synthesis of down-/up-conversion nanocomposites for dual-modal cell imaging and drug delivery. *Journal of Materials Chemistry B* **2**, 8372–8377 (2014).
39. Bagheri, A., Arandiyan, H., Boyer, C. & Lim, M. Lanthanide-Doped Upconversion Nanoparticles: Emerging Intelligent Light-Activated Drug Delivery Systems. *Advanced Science* **3** (2016).
40. Li, X. *et al.* Anisotropic encapsulation-induced synthesis of asymmetric single-hole mesoporous nanocages. *Journal of the American Chemical Society* **137**, 5903–5906 (2015).
41. Xu, Z. *et al.* Monodisperse core-shell structured up-conversion Yb(OH)CO₃@YbPO₄:Er³⁺ hollow spheres as drug carriers. *Biomaterials* **32**, 4161–4173 (2011).
42. Lu, S., Tu, D., Li, X., Li, R. & Chen, X. A facile ship-in-a-bottle approach to construct nanorattles based on upconverting lanthanide-doped fluorides. *Nano Research* **9**, 187–197 (2016).
43. Zhang, B. F., Frigoli, M., Angiuli, F., Vetrone, F. & Capobianco, J. A. Photoswitching of bis-spiropyran using near-infrared excited upconverting nanoparticles. *Chemical Communications* **48**, 7244–7246 (2012).
44. Dolmans, D. E., Fukumura, D. & Jain, R. K. Photodynamic therapy for cancer. *Nature reviews cancer* **3**, 380–387 (2003).
45. Castano, A. P., Mroz, P. & Hamblin, M. R. Photodynamic therapy and anti-tumour immunity. *Nature Reviews Cancer* **6**, 535–545 (2006).
46. Prasad, P. N. *Introduction to nanomedicine and nanobioengineering* (John Wiley & Sons, 2012).
47. Roy, I. *et al.* Ceramic-based nanoparticles entrapping water-insoluble photosensitizing anticancer drugs: A novel drug-carrier system for photodynamic therapy. *Journal of the American Chemical Society* **125**, 7860–7865 (2003).
48. Zhang, P., Steelant, W., Kumar, M. & Scholfield, M. Versatile photosensitizers for photodynamic therapy at infrared excitation. *Journal of the American Chemical Society* **129**, 4526–4527 (2007).
49. Wang, C., Tao, H., Cheng, L. & Liu, Z. Near-infrared light induced in vivo photodynamic therapy of cancer based on upconversion nanoparticles. *Biomaterials* **32**, 6145–6154 (2011).
50. Liu, J. *et al.* Magnetic and fluorescent Gd₂O₃:Yb³⁺/Ln³⁺ nanoparticles for simultaneous upconversion luminescence/MR dual modal imaging and NIR-induced photodynamic therapy. *International Journal of Nanomedicine* **12**, 1 (2017).
51. Zhu, X. *et al.* Temperature-feedback upconversion nanocomposite for accurate photothermal therapy at facile temperature. *Nature communications* **7** (2016).
52. Liu, B., Li, C., Xing, B., Yang, P. & Lin, J. Multifunctional UCNPs@PDA-ICG nanocomposites for upconversion imaging and combined photothermal/photodynamic therapy with enhanced anti-tumor efficacy. *Journal of Materials Chemistry B* **4**, 4884–4894 (2016).
53. Idris, N. M. *et al.* In vivo photodynamic therapy using upconversion nanoparticles as remote-controlled nanotransducers. *Nature medicine* **18**, 1580–1585 (2012).
54. Yang, G. *et al.* A Single 808 nm Near-Infrared Light-Mediated Multiple Imaging and Photodynamic Therapy Based on Titania Coupled Upconversion Nanoparticles. *Chemistry of Materials* **27**, 7957–7968 (2015).
55. Lim, M. E., Lee, Y.-I., Zhang, Y. & Chu, J. J. H. Photodynamic inactivation of viruses using upconversion nanoparticles. *Biomaterials* **33**, 1912–1920 (2012).
56. Nikfarjam, M., Muralidharan, V. & Christophi, C. Mechanisms of focal heat destruction of liver tumors. *Journal of Surgical Research* **127**, 208–223 (2005).
57. Wang, D. *et al.* New Advances on the Marrying of UCNPs and Photothermal Agents for Imaging-Guided Diagnosis and Therapy of Tumors. *Journal of Materials Chemistry B* (2017).

58. Fan, W. *et al.* Rattle-structured multifunctional nanotheranostics for synergetic chemo-/radiotherapy and simultaneous magnetic/luminescent dual-mode imaging. *Journal of the American Chemical Society* **135**, 6494–6503 (2013).
59. Karakoti, A. *et al.* Nanoceria as antioxidant: synthesis and biomedical applications. *JOM Journal of the Minerals, Metals and Materials Society* **60**, 33–37 (2008).
60. Young, L. S., Searle, P. F., Onion, D. & Mautner, V. Viral gene therapy strategies: from basic science to clinical application. *The Journal of pathology* **208**, 299–318 (2006).
61. Jayakumar, M. K. G., Idris, N. M. & Zhang, Y. Remote activation of biomolecules in deep tissues using near-infrared-to-UV upconversion nanotransducers. *Proceedings of the National Academy of Sciences* **109**, 8483–8488 (2012).
62. Boyer, J.-C. & Van Veggel, F. C. Absolute quantum yield measurements of colloidal NaYF₄: Er³⁺, Yb³⁺ upconverting nanoparticles. *Nanoscale* **2**, 1417–1419 (2010).
63. Cheng, L., Yang, K., Shao, M., Lee, S.-T. & Liu, Z. Multicolor in vivo imaging of upconversion nanoparticles with emissions tuned by luminescence resonance energy transfer. *The Journal of Physical Chemistry C* **115**, 2686–2692 (2011).
64. Wu, D. M., García-Etxarri, A., Salleo, A. & Dionne, J. A. Plasmon-enhanced upconversion. *The journal of physical chemistry letters* **5**, 4020–4031 (2014).
65. Medintz, I. L., Uyeda, H. T., Goldman, E. R. & Mattoussi, H. Quantum dot bioconjugates for imaging, labelling and sensing. *Nature materials* **4**, 435–446 (2005).
66. Li, Z., Zhang, Y. & Jiang, S. Multicolor core/shell-structured upconversion fluorescent nanoparticles. *Advanced Materials* **20**, 4765–4769 (2008).
67. Zou, W., Visser, C., Maduro, J. A., Pshenichnikov, M. S. & Hummelen, J. C. Broadband dye-sensitized upconversion of near-infrared light. *Nature Photonics* **6**, 560–564 (2012).
68. Cheng, L., Yang, K., Shao, M., Lu, X. & Liu, Z. In vivo pharmacokinetics, long-term biodistribution and toxicology study of functionalized upconversion nanoparticles in mice. *Nanomedicine* **6**, 1327–1340 (2011).
69. Gnach, A., Lipinski, T., Bednarkiewicz, A., Rybka, J. & Capobianco, J. A. Upconverting nanoparticles: assessing the toxicity. *Chemical Society Reviews* **44**, 1561–1584 (2015).
70. Altavilla, C. *Upconverting Nanomaterials: Perspectives, Synthesis, and Applications* (CRC Press, 2016).
71. Chen, C., Li, C. & Shi, Z. Current Advances in Lanthanide-Doped Upconversion Nanostructures for Detection and Bioapplication. *Advanced Science* **3** (2016).
72. Chithrani, B. D., Ghazani, A. A. & Chan, W. C. Determining the size and shape dependence of gold nanoparticle uptake into mammalian cells. *Nano letters* **6**, 662–668 (2006).
73. Wilhelm, S. *et al.* Analysis of nanoparticle delivery to tumours. *Nature Reviews Materials* **1**, 16014 (2016).